Synthesis and Characterization of Pyridine-Based Polybenzimidazoles for High Temperature Polymer Electrolyte Membrane Fuel Cell Applications[×]

L. Xiao[1,2], H. Zhang[1], T. Jana[1], E. Scanlon[1], R. Chen[1], E.-W. Choe[1], L. S. Ramanathan[1], S. Yu[1], and B. C. Benicewicz[1]*

[1] NYS Center for Polymer Synthesis, Department of Chemistry and Chemical Biology, Rensselaer Polytechnic Institute, Troy, NY 12180, USA

[2] Present address: PEMEAS USA-Fuel Cell Technologies, Cogswell Laboratory, Rensselaer Polytechnic Institute, Troy, NY 12180, USA

Received June 18, 2004; accepted November 16, 2004

Abstract

A series of polybenzimidazoles (PBIs) incorporating main chain pyridine groups were synthesized from the pyridine dicarboxylic acids (2,4-, 2,5-, 2,6- and 3,5-) and 3,3',4,4'-tetraaminobiphenyl, using polyphosphoric acid (PPA) as both solvent and polycondensation reagent. A novel process, termed the PPA process, has been developed to prepare phosphoric acid (PA) doped PBI membranes by direct-casting of the PPA polymerization solution without isolation or re-dissolution of the polymers. The subsequent hydrolysis of PPA to PA by moisture absorbed from the atmosphere usually induced a transition from the solution state to a gel-like state and produced PA-doped PBI membranes with a desirable suite of physiochemical properties. The polymer structure characterization included inherent viscosity (I.V.) determination as a measurement of polymer molecular weight and thermal stability assessment via thermogravimetric analysis. Physiochemical properties of the doped membrane were studied by measurements of the PA doping level, ionic conductivity and mechanical properties. The resulting pyridine-based polybenzimidazole membranes displayed high PA doping levels, ranging from 15 to 25 mol of PA per PBI repeat unit, which contributed to their unprecedented high proton conductivities of 0.1 to 0.2 S cm^{-1} at 160 °C. The mechanical property measurements showed that the pyridine-based PBI membranes were thermally stable and maintained mechanical integrity even at high PA doping levels. Preliminary fuel cell tests demonstrated the feasibility of the novel pyridine-based PBI (PPBI) membranes from the PPA process for operating fuel cells at temperatures in excess of 120 °C without any external humidification.

Keywords: Doping Level, Fuel Cell, High Temperature Polymer Electrolyte Membrane (PEM), Membrane Electrode Assembly (MEA), Phosphoric Acid (PA), Polybenzimidazole (PBI)

1 Introduction

Fuel cells based on solid polymer electrolytes have attracted much recent attention due to their promise as high energy density power sources for both mobile and stationary applications [1]. In particular, high temperature polymer electrolyte membranes operational above 120 °C without humidification offer many advantages including fast electrode kinetics, high tolerance to fuel impurities such as carbon monoxide and greatly simplified system design [2]. However, the current state-of-the-art perfluorosulfonic acid (PFSA)-based polymer electrolyte membranes such as Nafion® rely on the presence of water to solvate and transport the protons and therefore operate in a limited temperature range and require an elaborate water management system.

[×] *Article is part of Topical Issue 'Polymer Membranes'*

[*] *Corresponding author, benice@rpi.edu*

 DOI: 10.1002/fuce.200400067

Hence, much effort has gone into the development of low-cost, high performance and temperature-resistant alternative polymer electrolyte membranes for high temperature polymer electrolyte membrane fuel cells. Among various approaches developed so far, phosphoric acid (PA) doped polybenzimidazole (PBI) has emerged as a promising candidate for a low-cost and high performance fuel cell membrane material. It has been shown that this polymer electrolyte membrane exhibits high ionic conductivity at temperatures up to 200 °C, low gas permeability, excellent oxidative and thermal stability, and a nearly zero water drag coefficient [3–5]. However, further progress is still needed for the large scale application of PA-doped PBI fuel cell membranes.

The conventional method to prepare PA-doped PBI membranes involves first dissolving the commercially available PBI in an appropriate organic solvent, such as dimethyl acetamide (DMAc) with lithium chloride or trifluoroacetic acid (TFA)-based solvent mixture in a pressurized bomb reactor, then casting the film and subsequently doping the membrane with the desired PA electrolyte [6–8]. A wide range of membrane acid doping levels (3–16 mol of PA per PBI repeat unit) and proton conductivities (10^{-5}–0.13 S cm^{-1}) have been reported with the results varying from author to author due to various membrane preparation processes and various testing conditions [4, 9–12]. In general, the proton conductivities of the PA-doped PBI membranes increased with higher PA doping levels. For example, Bjerrum et al. reported a conductivity as high as 0.13 S cm^{-1} at 160 °C with a PA doping level of approximately 13~16 moles of PA per PBI repeat unit using the commercially available PBI with an I.V. of approximately 1.0 dL g^{-1} [13]. However, the mechanical properties of the membranes at high PA doping levels became poor and not suitable for membrane electrode assembly (MEA) fabrication [7, 14]. Based on the mechanical properties and the conductivity values, it was suggested that the appropriate PA doping levels should be 3.5–7.5 mol of PA per PBI repeat unit. Therefore, the membrane mechanical properties at high PA doping levels have become a major limiting factor for using the PA-doped PBI membranes from the conventional imbibing method for fuel cell applications.

One way to potentially improve the mechanical properties of the PA-doped PBI membranes with high proton conductivity and high PA doping level is to increase the molecular weight of the PBI polymers and to explore new membrane preparation methods. The current industrial standard process to produce the commercially available PBI employs a two-stage melt/solid-state polycondensation method. The I.V.s of the commercially available PBIs are limited to less than 1.2 dL g^{-1} as a result of the heterogeneous melt/solid-state polymerization. For example, the low molecular weight PBI (I.V. of 0.55~0.8 dL g^{-1}) was introduced under the trademark of "Celazole®", mainly for molding resin applications [15].

Polyphosphoric acid (PPA) has been widely used as an efficient condensation reagent for the synthesis of high I.V. rigid polybenzimidazoles in good yields [15–17]. Furthermore, polyphosphoric acid is extremely hygroscopic and will hydrolyze to phosphoric acid upon absorption of moisture. Although the synthesis of PBIs in PPA and aspects of the PA-doped PBI membranes for fuel cell applications have been investigated before, no successful attempts have been made to employ PPA as both polymerization medium and film casting solvent. Hence, we propose to employ polyphosphoric acid as polycondensation agent to prepare high molecular weight PBI polymers. In addition, PPA is a precursor to the phosphoric acid and may also serve as a casting solvent and facilitate the direct casting of the polymerization solution without isolation and/or re-dissolution of the PBI polymers. Overall, polyphosphoric acid may provide a unique opportunity to prepare high I.V. PBIs and yield the PA-doped PBI film with a desirable suite of properties in one step.

Among a variety of PBI structures, only limited types of PBIs, which included primarily the commercially available PBI, poly[2,2′-(m-phenylene)-5,5′-bibenzimidazole] (i.e., *m*-PBI), sulfonated or phosphorylated *m*-PBI as well as the poly(2,5-benzimidazole) (i.e., AB-PBI), have been explored for fuel cell applications [18]. No synthetic effort has been employed to systematically synthesize PBIs of different structures and study the effect of the PBI polymer molecular structure on the final film properties. Our present study aims to explore the opportunity of employing PPA to synthesize higher molecular weight PBIs with different molecular structures and study the effect of polymer structure on both film formation process and the final film properties. In particular, the substitution of pyridine dicarboxylic acids for the iso-/terephthalic acids will increase the number of basic groups in the polymers. A series of pyridine-based polybenzimidazole homopolymers were synthesized from tetraaminobiphenyl (TAB) and 2,4-, 2,6-, 2,5- and 3,5-pyridine dicarboxylic acids using PPA as both polycondensation reagent and film casting solvent. The polymer structure characterization included inherent viscosity (I.V.) determination as a measurement of polymer molecular weight and thermal stability assessment via thermogravimetric analysis. The physiochemical properties of the doped membranes were characterized by measurements of the PA doping level, mechanical properties and ionic conductivity. The preliminary fuel cell tests demonstrated the feasibility of the novel PBI membranes prepared from the PPA process for operating fuel cells at temperatures in excess of 120 °C without any external humidification or pressure requirements.

2 Experimental

2.1 Materials

Pyridine dicarboxylic acids (2,4-, 2,5-, 2,6- and 3,5- PDAs) were purchased from Acros Chemical (~98% purity) and purified by recrystallization from dilute hydrochloric acid prior to use. 3,3′,4,4′-Tetraaminobiphenyl (TAB, polymer grade) was donated by Celanese Ventures, GmbH and used as received. Polyphosphoric acid (115%) was used as supplied from Aldrich Chemical Co. and FMC Corporation.

2.2 Synthesis of PPBI Homopolymers

The general procedure for the synthesis of pyridine-PBIs (PPBIs) is described as follows: Purified pyridine dicarboxylic acid (12.534 g, 75 mmol) and TAB (16.074 g, 75 mmol) were added to a three-neck resin reaction flask in a nitrogen atmosphere glove box, followed by 200~400 g of polyphosphoric acid. The reaction mixture was stirred using a mechanical overhead stirrer and purged with a slow stream of nitrogen and the reaction temperature was controlled by a programmable temperature controller with ramp and soak features. The typical polymerization temperatures were approximately 190–220 °C for 16~24 h. During the polymerization, the reaction mixture became more viscous and developed a dark brown color. A small amount of the reaction mixture was poured into water and isolated as a brown mass. The mass was pulverized, neutralized with ammonium hydroxide, washed thoroughly with water, and dried in a vacuum oven for 24 h at 100 °C to obtain the pyridine PBIs for further characterization.

2.3 Film Formation

The polymer films were prepared by casting the polymerization solution directly onto glass plates using a film applicator with a gate thickness ranging from 0.127 mm (5 mil) to 0.635 mm (25 mil). The polyphosphoric acid solvent was hydrolyzed to phosphoric acid under controlled conditions (for example, by exposing films for 24 h at 25 °C and a relative humidity 40 ± 5%) to obtain polymer electrolyte membranes suitable for film properties and fuel cell testing.

2.4 Characterization Techniques

I.V.s of the polymer samples were measured at a polymer concentration of 0.2 g dL^{-1} in concentrated sulfuric acid (96%) at 30 °C, using a Cannon® Ubbelohde viscometer. Thermogravimetric analyses (TGA) in air and nitrogen were carried out on a Perkin-Elmer® TGA 7 or a Mettler-Toledo TGA/SDTA 851e at an air and nitrogen purging rate of 20 mL min^{-1} and a heating rate of 20 °C min^{-1}. Differential scanning calorimetry (DSC) tests were carried out on a Perkin-Elmer® DSC 7, a TA Instruments® DSC 2920, or a Mettler-Toledo® DSC 822e, with N_2 purging at a heating rate of 5 or 10 °C min^{-1}. The membrane PA doping levels were determined by titrating a piece of membrane sample with standard sodium hydroxide solution with a Metrohm® 716 DMS Titrino titrator. The samples were then washed with water, dried in a vacuum oven at 100 °C for 4 h to obtain the dry weight of polymer for the calculation of PA doping level. The PA doping levels, X, reported as moles of phosphoric acid per PBI repeat unit (PBI● X H_3PO_4) were calculated from the equation:

$$\text{PA doping level } X = (V_{NaOH}{}^{*}C_{NaOH})/(W_{dry}/M_w)$$

Where V_{NaOH} and C_{NaOH} are the volume and the molar concentration of the sodium hydroxide titer, while W_{dry} is the dry polymer weight and M_w is the molecular weight of the polymer repeat unit, respectively.

The membrane mechanical properties were tested utilizing a United® Tensile Tester (SSTM-1-PC) with a 22.2 N load cell. Dumb-bell specimens were cut following the ASTM standard D683 (Type V specimens). Tensile properties of all film samples were measured in an air atmosphere at room temperature with a cross head speed of 5 mm min^{-1}.

Through plane ionic conductivities were measured by a four-probe AC impedance method using a Zahner® IM6e spectrometer over a frequency range from 1 Hz to 100 KHz. A two-component model with a resistor in parallel with a capacitor was employed to fit the experimental curve of the membrane resistance across the frequency range. The conductivities of the membrane at different temperatures were calculated from the membrane resistance obtained from the ohmic resistance of the model simulation. Proton conductivity was then calculated from the following equation:

$$\sigma = D / (LBR)$$

where D is the distance between the two test current electrodes, L and B are the thickness and width, respectively, and R is the resistance value measured. The distance between the test electrode and sensor electrode was 2.0 cm.

3 Results and Discussion

3.1 Synthesis and Characterization of PPBI Homopolymers

The synthesis of pyridine-based homopolymers was investigated starting from tetraaminobiphenyl and pyridine dicarboxylic acids (2, 4-, 2, 6-, 2, 5- and 3, 5- PDAs) in polyphosphoric acid as shown in Scheme 1. Different diacid monomers gave different substitution patterns on the pyridine ring. For instance, the two carboxylic acid groups on 2,5-PDA are opposite to each other and give "*para*-orientation" while all the other monomers (3,5-, 2,6-, 2,4-) are of "*meta*-orientation".

There were some previous reports on the preparation of the pyridine-based PBIs in PPA that resulted in low I.V. pyridine-based PBI polymers or incomplete imidazole ring closure [19, 20]. In the present study, the initial polymerizations using diacid monomers without further purification gave PPBIs with I.V.s of less than 1.0 dL g^{-1}, as shown in Table 1.

Table 1 Inherent viscosity and polymerization data of PPBIs.

Polymer	Monomer purity	$\eta_{inh.}$ /dL g^{-1}	Polymerization concentration[a]
2,5-PPBI	As received	0.8	4%~18%
	Recrystallized	2.5-3.1	
3,5-PPBI	As received	0.6	4%~20%
	Recrystallized	1.3-1.9	
2,4-PPBI	As received	0.3	~7%
	Recrystallized	1.0	
2,6-PPBI	As received	0.2	~7%
	Recrystallized	1.3	

[a] Polymerization concentration: the wt.% of the final polymer.

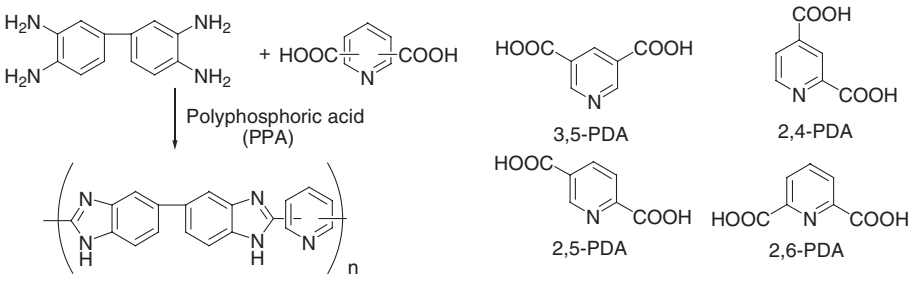

Scheme 1 Synthesis of PPBI hompolymers.

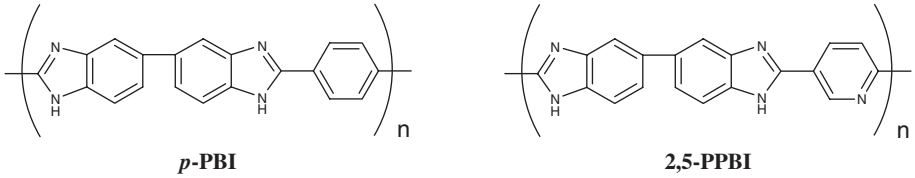

Scheme 2 The chemical structures of *p*-PBI and 2,5-PPBI.

Based on the Carother's equation, the monomer purity and accurate stoichiometry are crucial to obtain high I.V. polycondensation polymers. Therefore, a detailed study of the monomer purity and purification method was carried out on all the diacid monomers. DSC scans were employed to monitor the relative purity of the monomers and confirmed the improved monomer purity after purification. Table 1 shows that all diacid monomers polymerized to yield high I.V. pyridine-based PBIs after appropriate purification of starting materials and careful manipulation of polymerization conditions.

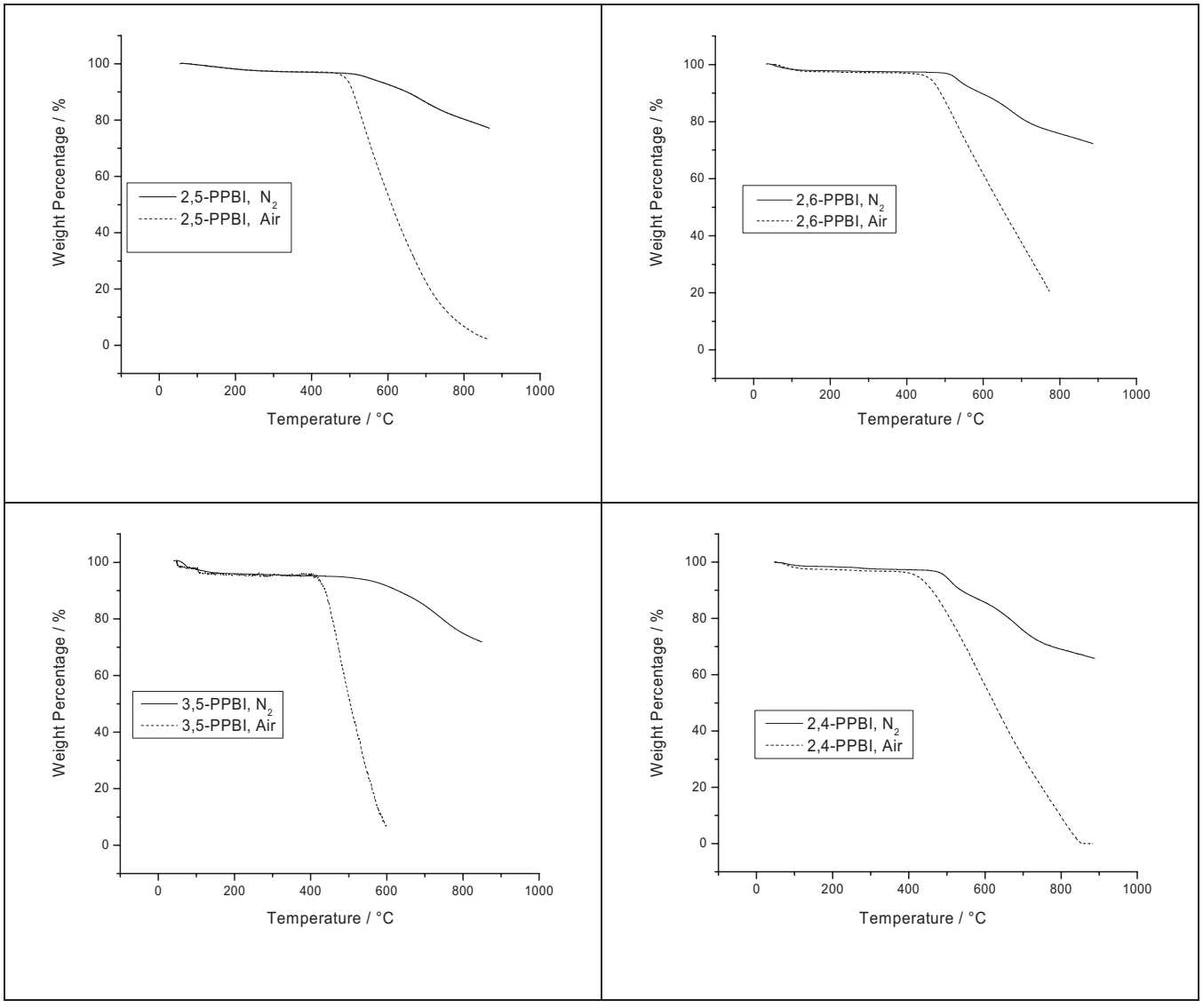

Fig. 1 Thermogravimetric analysis traces for PPBI polymers (20 °C min^{-1}).

One of the major barriers to the extensive application of the rigid rod PBI polymers has been their poor solubility and processability [16]. For example, the para-structure *p*-PBI, as shown in Scheme 2, has a rigid polymer backbone and limited solubility in polyphosphoric acid. The polymerizations of *p*-PBI in PPA are difficult to control at a polymerization concentration higher than 4% because the polymer precipitates [15, 21]. Surprisingly, the simple substitution of the pyridine ring for the phenyl ring allowed the polymerization of 2,5-PPBI in PPA at polymerization concentrations up to 18%. Clearly the incorporation of the extra nitrogen in the polymer backbone improved the solubility of the polymer in PPA significantly and thus enhanced the polymer processability.

The ^{1}H-NMR spectra of the PPBIs were measured in deuterated sulfuric acid (i.e. D_2SO_4). In all cases, the ^{1}H chemical shifts ranged from 7 to 9 ppm, confirming that all the protons were in aromatic environments. Signals that might be due to incomplete ring closure were not detected in any of the polymers synthesized in this work.

The TGA thermograms of the pyridine-based PBIs were obtained in both flowing nitrogen (20 mL min^{-1}) and flowing air (20 mL min^{-1}) at 20 °C min^{-1}, as shown in Figure 1. Analogous curves for all the other PPBI structures (2,4-, 2,6-) were similar and showed that the thermal stabilities of all the PPBIs were quite high with an initial decomposition temperature of approximately 420 °C in air, as expected from the characteristic wholly aromatic structures of the PPBI polymer backbone. Thus, it demonstrated that PPBI polymers incorporating main chain pyridine groups retained the inherently high thermo-oxidative stability of polybenzimidazoles.

3.2 Film Formation

In the present study, films of PPBI in polyphosphoric acid (PPA) were cast directly from the polymerization solution at approximately 200~220 °C without isolation or re-dissolution of the polymers. Since both polyphosphoric acid and PBI polymers were highly hygroscopic, moisture was readily absorbed from the atmosphere. The polyphosphoric acid solvent reacted with absorbed water to form phosphoric acid in-situ. The change in the nature of the solvent induced a sol-gel transition that produced membranes doped with phosphoric acid in one step. Furthermore, the effect of the polymer molecular structure on the film formation process was studied in detail, as summarized in Table 2, to understand and control the transition from solution to the desired gel films.

In the examples above, the polymerization concentration and subsequent casting concentration were adjusted for each polymer molecular structure, as shown in Table 2, to obtain a solution with an appropriate viscosity for film casting. The viscosities of the polymerization solution were a direct function of the rigidity of the polymer backbone, polymer concentration and polymer molecular weight. As shown in Table 2, the inherent viscosities of the 2,5-, 3,5-, 2,6-, 2,4- PPBIs were 2.5, 1.8, 1.3, and 1.0 dL g^{-1}, respectively, indicating reasonably high molecular weights. At the same polymerization concentration, the 2,5-PPBI polymerization solution was more viscous than all the other PPBI solutions due to its higher I.V. values and the more rigid polymer backbone stemming from the para-oriented 2,5-PDA diacid monomer.

In the case of the 2,5-PPBI, the hydrolysis of PPA to phosphoric acid coupled with the subsequent drain-off of the excess phosphoric acid and water increased the solid content and gave rise to mechanically strong polymer electrolyte membranes doped with phosphoric acid. This occurred in one step as opposed to the multiple steps of polymer isolation, redissolution in DMAc, film casting followed by washing, drying and PA doping that have been reported for the conventional imbibing method. When cast directly from a 4.5 wt.% 2,5-PPBI polymerization solution in PPA, mechanically strong PA-doped 2,5-PPBI membranes with a film solid content of approximately 7~8 wt.% were obtained. The PA doping levels of the resulting 2,5-PPBI membranes were approximately 15~25 mol of PA per PBI repeat unit, much higher than that of the previously reported PBI polymer electrolyte membranes prepared by the imbibing method which averaged 6 moles of phosphoric acid per PBI repeat unit.

In contrast, the 3,5-PPBI showed very different behavior when cast from the PPA polymerization solution (solid content 5~20%). The 3,5-PPBI polymer retained all of the phosphoric acid generated during the PPA hydrolysis process, and liquid drain-off was not observed. As a result, the 3,5-PPBI did not form a film upon casting from the PPA polymerization solution. Instead, the cast solution remained a honey-like solution upon hydrolysis of the polyphosphoric acid and a sol-gel transition was not observed.

The 2,4-PPBI with an I.V. of 1.0 dL g^{-1} was prepared in PPA and cast directly onto glass substrates. Upon hydrolysis, some liquid drain-off was observed. However, the mechanical properties of the resulting 2,4-PPBI films were extremely weak and the further characterization of the 2,4-PPBI membranes could not be performed because of the difficulty in maintaining film integrity.

Table 2 Effect of PPBI polymer structures on the film formation processes.

Sample	Diacid structure	I.V.	Cast conc. /wt.%	Film formation process
2,5-PPBI	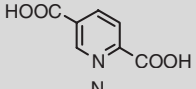	2.5	4.5%	Mechanically strong film
3,5-PPBI	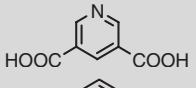	1.8	= 20%	No liquid drain-off, Not film-forming, honey-like solution
2,6-PPBI	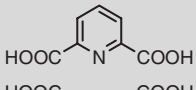	1.3	7.0%	Mechanically strong film
2,4-PPBI	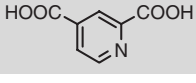	1.0	7.5%	Liquid drain-off Mechanically weak film

Mechanically strong PA-doped 2,6-PPBI membranes were prepared via the sol-gel process when cast directly from a 7.0 wt.% PPA polymerization solution. The 2,6-PPBI were the only meta-structure PPBI that gave strong membranes *via* the PPA process. The PA doping levels of the resulting membranes ranged from approximately 8 to 10 mol of PA per PPBI repeat unit with a polymer solid content of 15 wt.% to 20%, depending upon the hydrolysis process.

3.3 Membrane Properties

Further characterization of the pyridine-based PBI (PPBI) membranes from the PPA process involved determination of important fuel cell parameters such as the mechanical properties and the ionic conductivities.

The mechanical properties of the 2,5-PPBI and the 2,6-PPBI, as representatives of the *para*- and *meta*- structured pyridine-based PBI homopolymers, were characterized by tensile measurements. The typical stress-strain curves of the 2,5-PPBI and 2,6-PPBI membranes from the PPA process are shown in Figure 2 and summarized in Table 3.

In the case of 2,5-PPBI membranes from the PPA process, the PA doping level of the membranes averaged approximately 20 mol of phosphoric acid per PBI repeat unit, considerably higher than the previous reported values for PA-doped PBI membranes from the conventional imbibing method. The 2,5-PPBI membranes with such high PA doping levels were mechanically strong and easy to handle for the membrane electrode assembly (MEA) fabrication. An average tensile strength and elongation at break of about 1.8 MPa and 390% was obtained, respectively. In comparison, the previous literature indicated that the membrane mechanical properties became limiting at high PA doping levels and a useful doping level was suggested to be between 3.5 to 7.5 mol of PA per PBI repeat unit [13, 22].

The comparison between the mechanical properties of the 2,5-PPBI and 2,6-PPBI membranes clearly demonstrated that the different polymer molecular structures significantly affected the mechanical properties of the PPBI membranes from the PPA process. As shown in Figure 2, the 2,6-PPBI membranes from the PPA process exhibited mechanical properties quite different from those of the 2,5-PPBI membranes. The stress-strain curve of the 2,6-PPBI showed a yield stress of approximately 1.9 MPa at the yield strain of 40% and an ultimate tensile strength of about 1.8 MPa at an elongation of 150%. The elongation at break for the 2,6-PPBI membranes was considerably lower than that for the 2,5-PPBI membranes, probably because of the lower doping level of phosphoric acid and lower polymer I.V. values. The polymer weight percentages in the final 2,6-PPBI membranes were approximately twice as much as those for the 2,5-PPBI membranes, which were presumably due to the more flexible polymer backbone of the *meta*-structured 2,6-PPBI and the corresponding higher casting concentration.

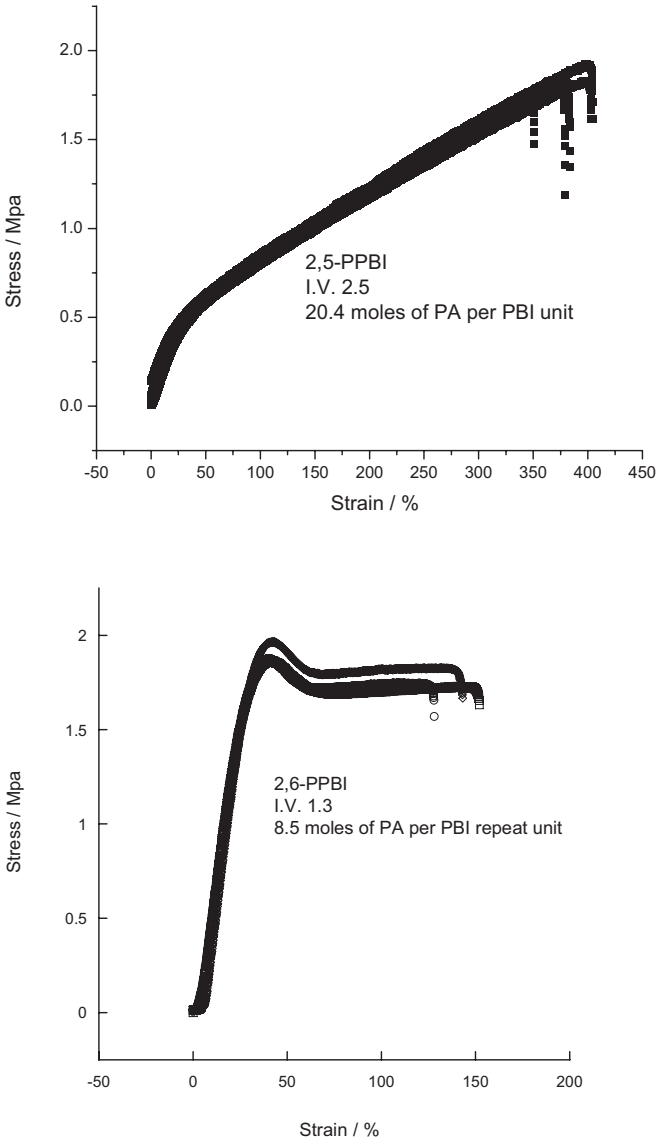

Fig. 2 Stress-strain curves of 2,5-PPBI and 2,6-PPBI membranes from the PPA process.

Overall, in contrast to the PA-doped PBI membranes from the conventional imbibing method, the PPBI membranes from the PPA process showed high mechanical properties at

Table 3 Comparison of tensile tests for 2,5-PPBI and 2,6-PPBI membranes from the PPA process.

Sample	Film composition / polymer wt.%	Yield stress / MPa(SD[a])	Yield strain / %(SD)	Stress at break / MPa(SD)	Strain at break / %(SD)
2,5-PPBI 2040 M%[b] PA doped	8.5%	0.45 (±0.03)	25.90 (±1.17)	1.82 (±0.09)	385.8 (±14.0)
2,6-PPBI 850 M% PA doped	17.8%	1.92 (±0.05)	42.90 (±1.47)	1.79 (±0.04)	153.0 (±19.7)

[a] SD: Standard deviation.
[b] PA doping level: molar percentage of PA per PBI repeat unit.

high PA doping levels owing to the high I.V. and unique gel structure of the polymers prepared *via* the PPA route. After casting film from the polymerization solution, the hydrolysis of the polyphosphoric acid to phosphoric acid induced a transition from solution to gel structure and generated high doping levels of phosphoric acid *in-situ*. The higher elongation at break for the *para*-structured 2,5-PPBI was influenced by the more rigid polymer backbone and higher polymer I.V. values which allowed the film casting at lower polymer concentrations and resulted in a higher PA doping level. The high PA doping level combined with high mechanical properties of the 2,5-PPBI membranes made the *para*-structured PPBI a promising candidate for fuel cell applications.

A key feature of a fuel cell membrane is its proton conductivity. It is well known that the proton conductivity of the PA-doped PBI membrane is greatly influenced by the presence of water and mildly dependent on the environmental humidity [23]. Furthermore, the operation of a PEMFC at temperatures higher than 120 °C without any external humidification is highly desired because it offers many advantages including alleviation of the water management problem, fast electrode kinetics and high tolerance to fuel impurities. As a result, fuel cell systems based on such high temperature membranes will be simplified considerably. Hence, the characterization of the membrane proton conductivities was focused on anhydrous conditions with temperatures ranging from room temperature to 200 °C. Since the PBI polymers are hygroscopic by nature due to the intermolecular hydrogen bonding between the N-H groups along the PBI backbone and water, the membranes were dried by first heating from room temperature to 200 °C and holding at 200 °C for 1 h. The membrane samples were then cooled in a vacuum oven and taken out just before the test in an effort to keep the samples dry. The proton conductivities for the PPBI polymer electrolyte membranes were measured as a function of temperature in a programmable drying oven, as reported in Figure 3 for 2,5-PPBI membranes and 2,6-PPBI membranes.

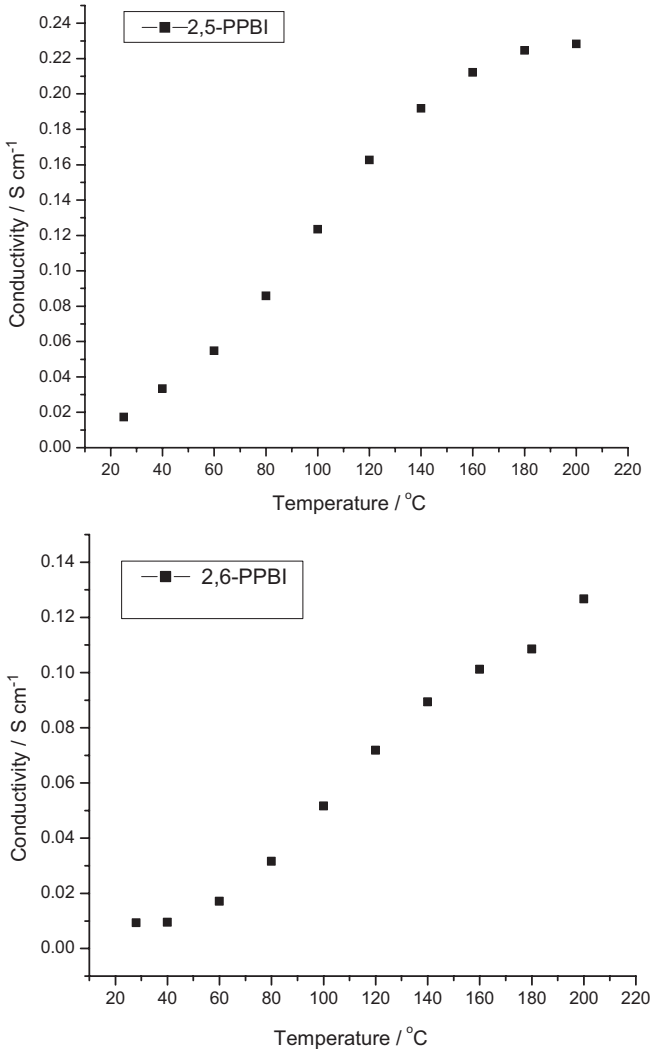

Fig. 3 Temperature dependence of ionic conductivity of PA-doped 2,5-PPBI and 2,6-PPBI membranes.

Figure 3 demonstrates that the conductivities of the PA-doped PBI membranes increased with temperature as well as the PA doping level. The *para*-structured 2,5-PPBI membrane with 20.4 mol of PA doping level exhibited a conductivity of 0.018 S cm^{-1} at room temperature and approximately 0.2 S cm^{-1} at 160–200 °C. For the *meta*-structured 2,6-PPBI membranes with 8.5 mol of PA doping level, the measured conductivity was 0.01 S cm^{-1} at room temperature and approximately 0.1 S cm^{-1} at 160–200 °C. The comparison between the proton conductivities of the 2,5-PPBI membranes and 2,6-PPBI membranes confirmed that the polymer molecular structure and doping levels affected the properties of the final membranes significantly. The only difference between the 2,5- and 2,6-PPBI membranes was the substitution pattern on the incorporated pyridine ring which varied the rigidity of the polymer backbone, the viscosity of the casting solution and the PA doping level of the final membranes.

In comparison, the previously reported conductivity values for the PA-doped *m*-PBI (commercial PBI structure) membranes ranged from 2.5×10^{-3} S cm^{-1} at 130 °C for a membrane with PA doping level of 380 mol% H_3PO_4 to 4.6×10^{-2} S cm^{-1} at 165 °C for a membrane doped with 450 mol% H_3PO_4 [7, 22]. Despite the variations in the physical and chemical differences between the PA-doped 2,5-PPBI and 2,6-PPBI membranes, the proton conductivities of both PPBI membranes are considerably higher than those reported previously for the PA-doped PBI membranes prepared via the conventional imbibing method owing to their inherently high PA doping levels. More importantly, these highly conductive PPBI membranes from the PPA process were mechanically strong at the high PA doping level and therefore amenable for MEA fabrication.

A better understanding of the mechanism for the membrane proton conductivity can be obtained from the Arrhenius plot of the ln (σT) against the inverse of temperature. In a proton-hopping dominant mechanism, the conductivity usually follows a simple Arrhenius law as described by the equation:

$$\sigma = \sigma_0 \exp\left(-\frac{Ea}{RT}\right)$$

where Ea is an activation energy for conduction, σ_0 is a pre-exponential factor and R is the gas constant. A straight line in this type of plot usually indicates an Arrhenius type of behavior while changes in the slope of the curves imply a much more complicated mechanism. Figure 4 presents the Arrhenius plots of the 2,5-PPBI and 2,6-PPBI membranes.

The temperature dependence of the conductivity for both membranes showed a straight line for the temperature range from room temperature to approximately 160 °C, as demonstrated by the linear curve fitting shown in Figure 4. However, the slopes of the curves decreased and deviated from the straight line at temperatures higher than 160 °C, which indicated a more complicated mechanism.

When curvature is present in the plots of ln (σT) against $1/T$, empirical equations derived from free-volume theory such as the Vogel-Tamman-Fulcher equation and Williams-Landel-Ferry equation are usually employed to explain the mechanism. However, in our case, another hypothesis that may account for the curvature is the composition change of the phosphoric acid. It has been suggested that the proton conduction mechanism in the PA-doped PBI may be attributed to conduction through a chain of acid molecules as well as the interaction of PBI polymers and the phosphoric acid [23]. The phosphoric acid protonates the imidazole ring of the PBI polymers and the protons hop between the PBI backbones and the acid facilitated by the hydrogen bond forming and breaking processes. Higher temperatures enhance the Brownian motion and contribute to faster proton switching processes, which provide an explanation for the overall trend of increasing conductivity with increasing temperatures for the PA-doped PBI membrane systems. A counter effect of the increasing temperature at temperatures higher than 160 °C is the formation of the oligomeric species of polyphosphoric acid which results in lower proton conductivity [24]. Further detailed study of the proton conduction mechanism employing solid state NMR technique is in progress and will be presented in a subsequent research article.

Overall, the pyridine-based PBI membranes from the PPA process exhibit excellent mechanical properties and proton conductivity at high temperatures and are promising materials for high temperature PEM fuel cell applications. Preliminary fuel cell evaluations were performed on the 2,5-PPBI membrane from the PPA process with a thickness of 0.203 mm (~8 mils), as illustrated in Figure 5. The MEA active area was 10 cm^2 and noble metal (Pt) catalyst loading in both electrodes was 1.0 mg cm^{-2}. It should be noted that all PBI-based fuel cells were operated without external humidification for either hydrogen or oxygen. The results showed that the PA-doped PBI membranes prepared from the PPA process can be used successfully for operating a fuel cell at tem-

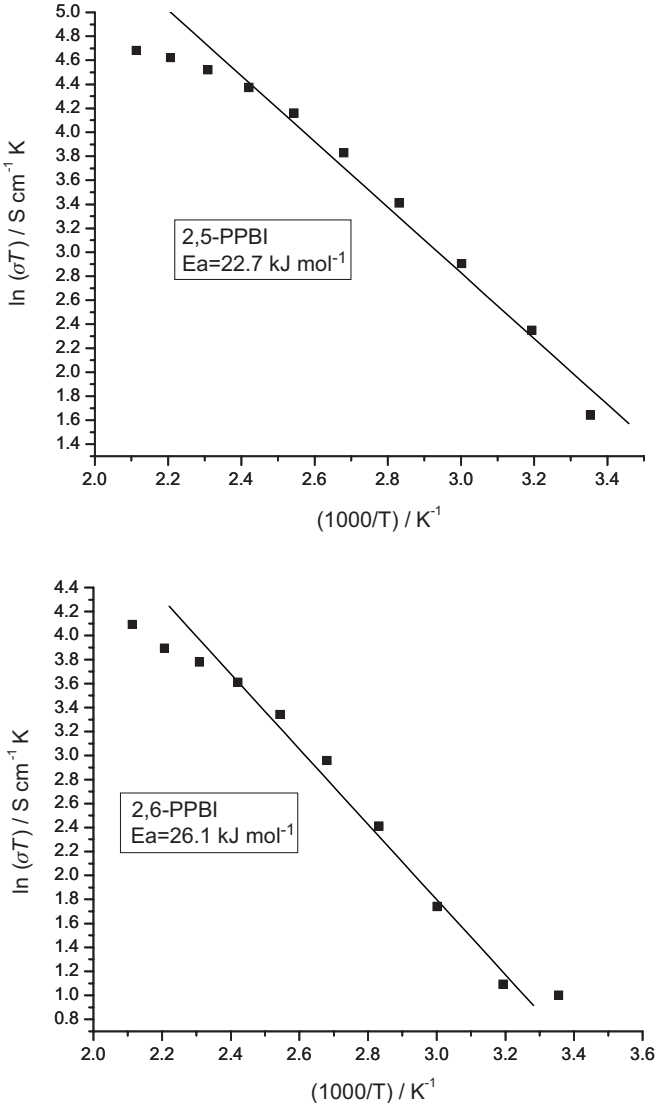

Fig. 4 Arrhenius plots of ln (σT) *vs.* $1/T$ of 2,5-PPBI membrane and 2,6-PPBI membranes prepared from the PPA process.

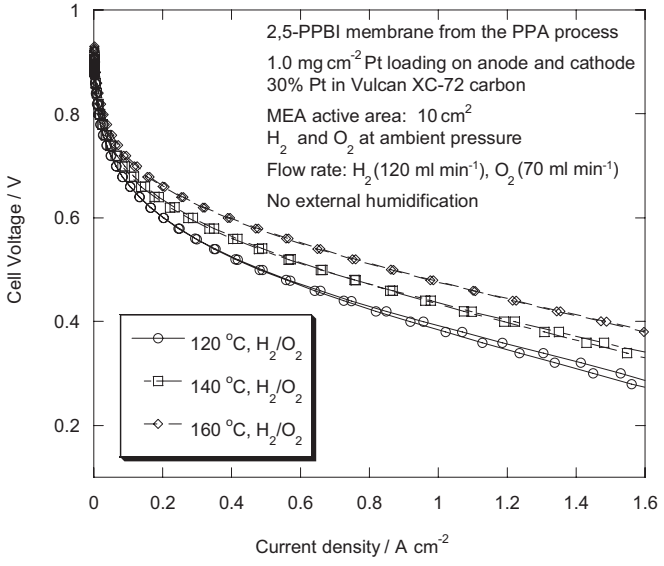

Fig. 5 Performance curves of H_2/O_2 fuel cells based on PA-doped PPBI membranes from the PPA process.

peratures in excess of 120 °C without any external humidification or pressure requirements. As seen from Figure 5, higher operational temperatures provided better cell performance. The optimization of film composition and the membrane electrode assembly (MEA) fabrication technique is in progress. Further characterization of the fuel cell performance using the PA-doped PBI membranes from the PPA process with different polymer backbone structures will be discussed in future publications.

4 Conclusions

A series of polybenzimidazoles (PBIs) incorporating main chain pyridine groups were synthesized using polyphosphoric acid (PPA) as both solvent and polycondensation reagent. After appropriate purification of starting materials and optimization of polymerization conditions, all pyridine dicarboxylic acid monomers (3,5-, 2,5-, 2,4- and 2,6- PDAs) polymerized with TAB to yield high I.V. pyridine-based polybenzimidazoles with properties influenced by the substitution pattern on the pyridine ring. The incorporation of the pyridine group as an additional nitrogen-containing aromatic heterocycle increased the base content of the polymer while retaining the inherently high thermo-oxidative stability of the polybenzimidazoles. The results also suggested that the incorporation of pyridine groups as an additional nitrogen containing heterocycle enhanced the interaction of phosphoric acid and the polymer.

In comparison with the PBI membranes cast from DMAc organic solvent and subsequently imbibed with phosphoric acid, the PA-doped PBI polymer electrolyte membranes prepared via the PPA process possessed high PA loading levels with good mechanical properties and enhanced proton conductivities. It was shown that the polymer molecular structures affected the properties of the polymers and the corresponding film formation process significantly. Among four types of PPBI homopolymers, the *para*-structured 2,5-PPBI gave mechanically strong membranes with a high PA doping level of approximately 20 mol of PA per PBI repeat unit, which contributed to its unprecedented high proton conductivities of approximately 0.2 S cm^{-1} at 200 °C. Furthermore, Arrhenius type behavior confirmed that the proton conduction mechanism in the PA-doped PBI was consistent with a conduction mechanism through a chain of acid molecules as well as the interaction between PBI polymers and phosphoric acid. Preliminary fuel cell tests have demonstrated the feasibility of the novel pyridine-based PBI membranes from the PPA process for operating a fuel cell at temperatures in excess of 120 °C without any external humidification or pressure requirements.

Acknowledgements

The authors thank PEMEAS GmbH for financial and technical support and Plug Power Inc. for assistance in fuel cell testing methods. NYSTAR is gratefully acknowledged for partial support in establishing The Fuel Cell Test Laboratory at Rensselaer. We also acknowledge receipt of the 2001 Mettler-Toledo Thermal Analysis Education Grant in honor of Professor Edith Turi.

References

[1] B. C. H. Steele, A. Heinzel, *Nature* **2001**, *414*, 345.
[2] C. Yang, P. Costamagna, S. Srinivasan, J. Benziger, A. B. Bocarsly, *J. Power Sources* **2001**, *103*, 1.
[3] R. Savinell, E. Yeager, D. Tryk, U. Landau, J. Wainright, D. Weng, K. Lux, M. Litt, C. Rogers, *J. Electrochem. Soc.* **1994**, *141*, L46.
[4] J. S. Wainright, J. T. Wang, D. Weng, R. F. Savinell, M. Litt, *J. Electrochem. Soc.* **1995**, *142*, L121.
[5] D. Weng, J. S. Wainright, U. Landau, R. F. Savinell, *Proc. – Electrochem. Soc.* **1995**, *95–23*, 214.
[6] J. T. Wang, R. F. Savinell, J. Wainright, M. Litt, H. Yu, *Electrochim. Acta* **1996**, *41*, 193.
[7] R. F. Savinell, M. H. Litt, *WO Patent 9737396*, Case Western Reserve University, USA, **1997**.
[8] J. S. Wainright, R. F. Savinell, M. H. Litt in *Proceedings of the International Symposium on New Materials for Fuel Cell and Modern Battery Systems, 2nd, Montreal* **1997**, p. 808.
[9] Y. L. Ma, J. S. Wainright, M. H. Litt, R. F. Savinell, *J. Electrochem. Soc.* **2004**, *151*, A8.
[10] M. Kawahara, J. Morita, M. Rikukawa, K. Sanui, N. Ogata, *Electrochim. Acta* **2000**, *45*, 1395.
[11] M. Litt, R. Ameri, Y. Wang, R. Savinell, J. Wainwright, *Mater. Res. Soc. Symp. Proc.* **1999**, *548*, 313.
[12] X. Glipa, B. Bonnet, B. Mula, D. J. Jones, J. Roziere, *J. Mater. Chem.* **1999**, *9*, 3045.
[13] Q. Li, H. A. Hjuler, N. J. Bjerrum, *Journal of Appl. Electrochem.* **2001**, *31*, 773.
[14] W. F. Lin, J. T. Wang, R. F. Savinell, *J. Electrochem. Soc.* **1997**, *144*, 1917.
[15] E. W. Choe, D. D. Choe in *Polymeric Materials Encyclopedia, Vol. 7* (Ed. J. C. Salamone), CRC Press, New York, **1996**, p. 5619.
[16] R. Twieg, T. Matray, J. L. Hedrick, *Macromolecules* **1996**, *29*, 7335.
[17] A. B. Conciatori, E. W. Choe, H. K. Hall, Jr., *US Patent 4414383*, Celanese Corp., USA, **1983**.
[18] M. A. Hickner, H. Ghassemi, Y. S. Kim, B. R. Einsla, J. E. McGrath, *Chemical Reviews* **2004**, *104*, 4587.
[19] T. Brock, D. C. Sherrington, H. G. Tang, *Polymer* **1991**, *32*, 353.
[20] A. H. Gerber, *US Patent 3741938*, Horizons Research, Inc., USA, **1976**.
[21] Y. Iwakura, K. Uno, K. Nume, *US Patent 3741938*, Maruzen Oil Co., Ltd., **1973**.
[22] J. T. Wang, J. Wainright, H. Yu, M. Litt, R. F. Savinell, *Proc. – Electrochem. Soc.* **1995**, *95–23*, 202.
[23] A. Schechter, R. F. Savinell, *Solid State Ionics* **2002**, *147*, 181.
[24] M. Kawabe, O. Ohashi, I. Yamaguchi, *Bull. Chem. Soc. Jpn.* **1970**, *43*, 3705.

